



X-ray diffraction study of multiphase reverse reaction with molten CuCl and oxygen

G.D. Marin, Z. Wang, G.F. Naterer*, K. Gabriel

Faculty of Engineering and Applied Science, University of Ontario Institute of Technology, 2000 Simcoe Street North, Oshawa, Ontario, Canada L1H 7K4

ARTICLE INFO

Article history:

Received 8 March 2011

Received in revised form 30 June 2011

Accepted 1 July 2011

Available online 7 July 2011

Keywords:

Hydrogen production

Reverse reaction

Molten salt

X-ray diffraction

ABSTRACT

The thermochemical copper–chlorine (Cu–Cl) cycle for hydrogen production includes three chemical reactions of hydrolysis, decomposition and electrolysis. The decomposition of copper oxychloride for oxygen production establishes the high-temperature limit of the cycle. At 450–530 °C, copper oxychloride (Cu_2OCl_2) decomposes to produce a molten salt of cuprous chloride (CuCl, copper I chloride) and oxygen gas. Minimization of the reverse reaction and undesirable products is critical for the proper operation of the Cu–Cl cycle. This paper examines the operating conditions that disfavor the reverse reaction of the oxygen production, and the parameters that maximize the extent of the forward reaction. Experiments were designed to disperse oxygen gas into a molten CuCl bath to study its reaction at 450–500 °C. The composition of the products was quantified with X-ray diffraction measurements. Experimental results indicate that a high decomposition extent of copper oxychloride is obtained at equilibrium when the temperature is higher than 500 °C, and the oxygen pressure is below 2 bar. The thermochemistry data of the reactants and products were also determined and reported. These thermodynamic data provide a key missing gap in the understanding of the Cu–Cl cycle of thermochemical hydrogen production. The data includes the standard formation entropy, enthalpy and Gibbs free energy at different temperatures. Also, in this paper, a thermodynamic analysis is performed to investigate the reverse reaction from the aspects of spontaneity and optimization of the operating parameters. It is found that the optimal operating parameters for minimizing the reverse reaction lie in the pressure range of 1–2 bar and a temperature range of 500–525 °C.

© 2011 Elsevier B.V. All rights reserved.

1. Introduction

Hydrogen is a promising future clean fuel and also a necessity for numerous existing industries such as petrochemicals, fertilizers and increasingly as a future transportation fuel. Conventional hydrogen production technologies require the utilization of primary energy sources in the form of electricity, natural gas, coal, oil, biomass or others that emit greenhouse gases. The predominant existing process is steam methane reforming (SMR) [1].

Researchers have endeavored to develop alternate hydrogen production methods that can split water by using clean energy sources, and consequently lower greenhouse gas emissions. Thermochemical hydrogen production is a technology that produces hydrogen through a cycle of chemical and physical processes for the overall splitting of water. McQuillan et al. [1] surveyed and compared over 200 cycles for thermochemical hydrogen production based on stoichiometric and energy requirements. A literature

search in the 1970s and early 1980s resulted in the identification of several promising thermochemical cycles including S–I, Cu–Cl, Cu–SO₄, and Zn–SO₄ cycles. Carty et al. [2] performed an analysis of processes of hydrogen production based on the criteria of reactions whose free energy change lies within 10 kcal for a given temperature. Lewis and Taylor [3] applied these criteria, in addition to the advantages of relatively low temperature (≤ 600 °C) operation, high efficiency, and materials requirements, to recommend six cycles of hydrogen production. Among the most promising cycles, the Cu–Cl cycle has the lowest temperature requirement that can be supplied by the temperatures of SCWR (Supercritical Water-cooled Reactor) and current solar thermal plant technology. Furthermore, due to the lower temperature requirement of the Cu–Cl cycle, its industrialization would be anticipated to have fewer material challenges than other higher temperature cycles [4,5].

The processes of the Cu–Cl cycle are shown in Fig. 1. The three reactions and their key parameters are described in Table 1. The oxygen production reaction involves the decomposition of Cu_2OCl_2 to produce molten CuCl and oxygen gas in a forward reaction. Past studies by Zamfirescu et al. [6], Daggupati et al. [7] and Haseli et al. [8] have reported the characteristics of various copper chlo-

* Corresponding author. Tel.: +1 905 721 8668; fax: +1 905 721 3370.
E-mail address: greg.naterer@uoit.ca (G.F. Naterer).

Nomenclature

B	bias
C_p	specific heat capacity at constant pressure (J/mol K)
d	distance of atomic layers in the crystal (m)
G_i	Gibbs energy of species i (kJ/mol)
$\Delta_f^T G$	standard free Gibbs energy of reaction at temperature T (J/mol)
H	enthalpy (J)
$\Delta_f H$	enthalpy of formation (J/mol)
K	equilibrium constant
k_0	pre-exponential factor
\dot{m}	molar rate (mol/s)
n_i	moles of species i (mol)
n	integer, multiplier of wavelengths
P	pressure (bar)
P_m	precision
p_{O_2}	partial pressure of oxygen (bar)
Q	reaction quotient
R	universal gas constant (J/mol K)
S	entropy (J/mol K)
T_i	initial temperature of reactants (K)
T_{sp}	target temperature (K)
T_r	reactor temperature (K)
U	overall uncertainty

Chemical compounds

CuCl	cuprous chloride
CuCl ₂	cupric chloride
CuO	copper oxide
CuOHCl	copper hydroxide chloride
Cu ₂ OCl ₂	copper oxychloride
HCl	hydrogen chloride

Greek symbols

λ	wavelength of incident X-rays
θ	angle of diffraction

sirable products is particularly critical to the integration of the Cu–Cl cycle.

Studies on this potential reverse reaction of the oxygen production process have not been reported in past literature. Although the reaction of CuCl and oxygen to produce Cu₂OCl₂ has been reported previously for the synthesis of a catalyst (CuCl + 1/2O₂ = Cu₂OCl₂), it was a theoretical study on the reaction mechanism and not verified by experiments [9]. Copper oxychloride is not commercially available and it exists in nature in very few locations as a mineral called melanothallite. In past reported studies, it was prepared in a laboratory through a lengthy process that utilized an equimolar mixture of copper oxide (CuO) and cupric chloride (CuCl₂ or copper II chloride) in a quartz tube vacuum heated for several days at 400 °C to synthesize Cu₂OCl₂ [10]. The synthesis was performed by utilizing CuCl₂ and CuO rather than CuCl and O₂. However, an experimental verification of the reverse reaction of the oxygen production process has not been reported in the past. The extent of decomposition of Cu₂OCl₂ was reported for a small sample of 0.01–0.02 mol of Cu₂OCl₂ that was heated to 530 °C [11,12]. The results indicated that the oxygen yield can exceed 85%.

A two-stage reaction mechanistic analysis assumed that the overall oxygen generation reaction was limited by the chemical bond splitting of CuCl₂ of the Cu₂OCl₂ crystal [12]. But the reverse reaction was not measured because the sample amounts in the experiments were so small as to be unable to measure and observe the reverse reaction. This paper will present an experimental study of the reverse reaction from the perspectives of optimization of operating conditions and reaction extent, so as to minimize the reverse reaction and undesirable products. The thermochemical properties such as the standard formation entropy, enthalpy and Gibbs free energy at different temperatures for Cu₂OCl₂ and CuCl will be determined for the oxygen production process of the Cu–Cl cycle. Then a thermodynamic analysis will be performed to study the reverse reaction from the aspects of spontaneity and optimization of the operating parameters.

2. Experimental configuration

The experimental loop for the reverse reaction is shown in Fig. 2. The reactor contains a crucible that can withstand a very high temperature and it is chemically inert to both solid and molten CuCl. The crucible contains the sample and holds the probes for air injection and temperature measurement. It is located inside of a heating chamber surrounded by the top heating zone of the furnace, a vertical split tubular furnace consisting of three separate heating zones that can provide a stable temperature in the range of 50–1000 °C by adjusting the input power to each zone. The inside diameter of the crucible varies from 5 to 20 cm so as to study the influence of the CuCl quantity and mixing. The heating chamber also provides secondary containment and it is used to purge the reaction environment from humidity and oxygen by using nitrogen. The entire assembly is placed inside the furnace. Nitrogen is injected and allowed to flow in order to obtain the desirable oxygen fraction for the reverse reaction.

The bottom temperature of the molten CuCl in the reactor was measured by type K thermocouples with a 4–20 mA transmitter programmed for 30–1000 °C. The uncertainty of the output is ±0.1% of the span that is equivalent to ±0.97 °C. A mixture of oxygen and nitrogen is utilized as the oxygen source for the reactant of the reverse reaction. In the experiments, solid CuCl is fed into the reactor and heated to a molten state, and then air is bubbled through the molten CuCl at various temperatures. The gases exiting the heating chamber are cooled down to ambient temperature via a heat exchanger. The gases are then sampled continuously with an oxygen analyzer for the instantaneous oxygen concentration analysis.

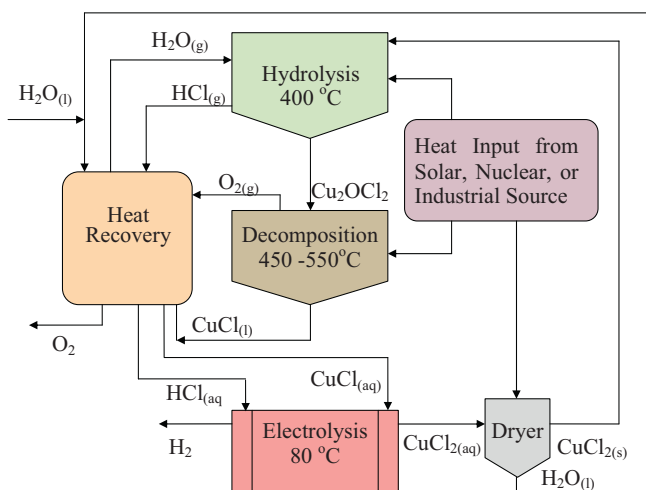


Fig. 1. Schematic of the thermochemical copper–chlorine cycle.

ride compounds in the Cu–Cl cycle, including molten and vapor CuCl. There may exist a reverse reaction in the decomposition of Cu₂OCl₂, for example, with molten CuCl reacting with oxygen to produce Cu₂OCl₂. Minimization of this reverse reaction and unde-

Table 1
Reactions in the thermochemical Cu–Cl cycle.

Reaction	Process	T (°C)	Enthalpy change (kJ/mol)
$\text{CuCl}(\text{aq}) + \text{HCl}(\text{aq}) \rightarrow \text{CuCl}_2(\text{aq}) + (1/2) \text{H}_2(\text{g})$	Electrolysis (hydrogen production)	80–100	93.7 electrolytic
$2\text{CuCl}_2(\text{s}) + \text{H}_2\text{O}(\text{g}) \rightarrow \text{Cu}_2\text{OCl}_2(\text{s}) + 2\text{HCl}(\text{g})$	Hydrolysis (water splitting)	340–400	116.7 endothermic
$\text{Cu}_2\text{OCl}_2(\text{s}) \leftrightarrow (1/2) \text{O}_2(\text{g}) + 2\text{CuCl}(\text{molten})$	Decomposition (oxygen production)	450–550	129.3 endothermic
Sum: $\text{H}_2\text{O}(\text{g}) = \text{H}_2(\text{g}) + (1/2) \text{O}_2(\text{g})$			

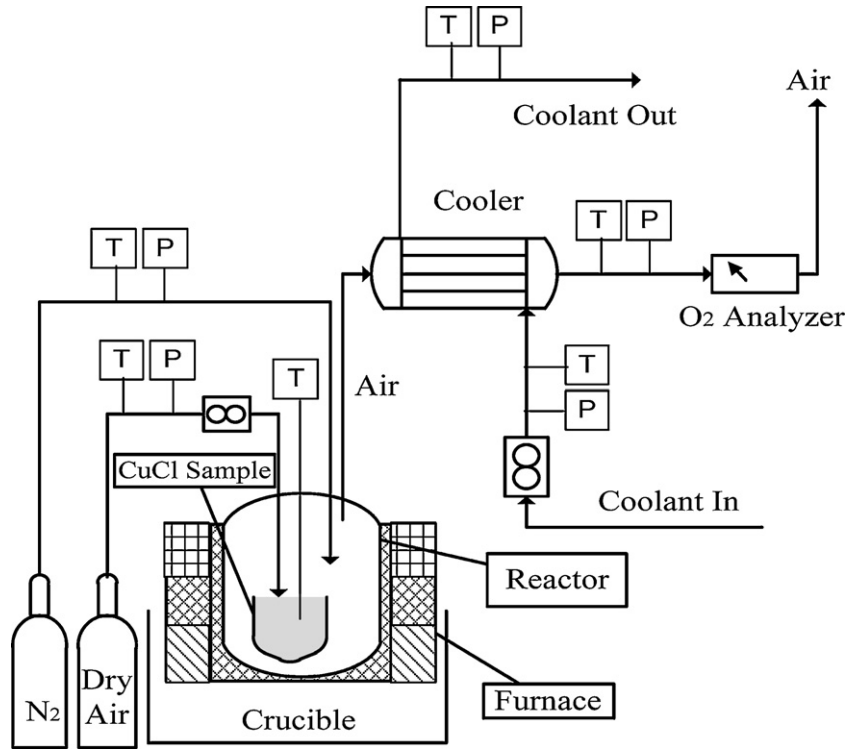


Fig. 2. Experimental configuration for the reverse reaction of molten CuCl and O₂.

The oxygen analyzer, AMI-201RSP, has four volumetric measurement spans of 0–1%, 0–5%, 0–10% and 0–100%. The uncertainty is $\pm 1\%$ of the selected span, or equivalent to $\pm 0.01\%$ of the oxygen volumetric fraction when the span is set at 0–1%. The concentration of oxygen from the reactor is also measured with the oxygen analyzer before the experiments, allowing for measurement of the oxygen concentration decrease that is caused by its reaction with molten CuCl in the experiments. The total quantity of reacted oxygen can be determined from integration of the concentration curve and the flow rates of air and nitrogen. The flow rates of air and nitrogen are controlled continuously, and the values are monitored in a real-time mode. The flow controllers, Omega FVL2600, have an uncertainty of $\pm 0.8\%$ of the full scale. Three flow controllers are utilized in order to approach various flow rates in the range of 0–100 sccm, 0–2 slm, and 0–50 slm. The oxygen quantity was calculated by assuming ideal behavior as follows:

$$\dot{m}_{\text{O}_2} = \frac{1}{22.4} (p_{\text{O}_2}) (F_{\text{N}_2}) \left(\frac{P_1 T_2}{P_2 T_1} \right) \quad (1)$$

In this equation, P_1 , T_1 and P_2 , T_2 represent the pressure/temperature at the inlet and outlet conditions, respectively. Also, p_{O_2} , F_{N_2} and \dot{m}_{O_2} represent the partial pressure of oxygen, flow of nitrogen and mass flow of oxygen, respectively. The uncertainty of the total mol evolution was determined by following a combination of a precision (random) contribution to the uncertainty of \dot{m} , P_m , and a bias contribution to the uncertainty of \dot{m} , B_m . The two contributions can be evaluated separately in terms of the

sensitivity of coefficients based on the Kline and McClintock equation [13] for error propagation:

$$p_m^2 = \left(\frac{\partial \dot{m}}{\partial p} \right)^2 p_p^2 + \left(\frac{\partial \dot{m}}{\partial T} \right)^2 p_T^2 + \left(\frac{\partial \dot{m}}{\partial A_{\text{O}_2}} \right)^2 p_{A_{\text{O}_2}}^2 + \left(\frac{\partial \dot{m}}{\partial F_{\text{N}_2}} \right)^2 p_{F_{\text{N}_2}}^2 \quad (2)$$

and

$$B_m^2 = \left(\frac{\partial \dot{m}}{\partial p} \right)^2 B_p^2 + \left(\frac{\partial \dot{m}}{\partial T} \right)^2 B_T^2 + \left(\frac{\partial \dot{m}}{\partial A_{\text{O}_2}} \right)^2 B_{A_{\text{O}_2}}^2 + \left(\frac{\partial \dot{m}}{\partial F_{\text{N}_2}} \right)^2 B_{F_{\text{N}_2}}^2 \quad (3)$$

The overall uncertainty in the determination of the total oxygen evolution is expressed by:

$$U = (p_m^2 + B_m^2)^{1/2} \quad (4)$$

where the subscripts p , T , A_{O_2} , F_{N_2} of precision (P) and bias (B) represent pressure, temperature, percent analyzer reading and flow meter, respectively; and U represents the overall uncertainty. Uncertainty estimates were taken over a representative period of the experiments. Experiments were repeated under similar conditions of initial mass and molar ratios, initial weight, reactor pressure and purge gas flow. A steady set of data was selected over a period for the uncertainty calculations. The measured uncertainty of moles of percent volume oxygen reading was determined as 1.87%, based on precision (random) contributions to the uncertainty of \dot{m} , P_m and a bias contribution to the uncertainty of \dot{m} , B_m . The fit of XRD

data compared to data from the International Centre for Diffraction Data and inaccuracies introduced by the Rietveld method result in a weighted *R*-factor of approximately 3% in the phase determination. The composition of the reverse reaction product is analyzed by an X-ray diffraction (XRD) technique after solidification of CuCl. The Bragg's Law of XRD diffraction is represented as follows:

$$n\lambda = 2d \sin(\theta) \quad (5)$$

The equation describes how the cleavage face of crystals reflects X-ray beams at certain angles of incidence. When the angle of incidence θ equals the angle of scattering, and the path-length difference equals an integer number of wavelengths n , then peaks of scattered intensity can be observed [14–16]. In the equation, d represents the distance between atomic layers in the crystal. λ , is the known wavelength of incidence of the X-ray beams and n is an integer.

Bragg's Law conditions occur at a different d -spacing in materials with a polycrystalline structure. A pattern can then be obtained by plotting the angular positions and intensities of the resultant diffracted peaks of radiation. The diffracted peaks are a characteristic that depends exclusively on the crystalline structure of the sample. If the sample contains a mixture of different phases, the pattern shows the reflections of individual phase characteristics at different angular positions. Powder diffraction XRD was applied to a 1 mm thick sample in a 2 cm² bed in order to characterize the crystallographic structure. The measurements used a Philips PW 1830HT generator with a PW1050 goniometer, PW3710 control, X-pert software (2007 version; International Centre for Diffraction Data) and Rietveld refinement software. In the XRD analysis of the CuCl samples, the angle 2θ was allowed to vary within a range of 5–60°.

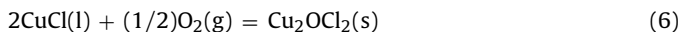
Two purity grades of CuCl were used for the reactant, i.e., analytical grade for thermodynamic analysis, and industrial (assay 99%) for simulating the effects of trace amounts of impurities on the reverse reaction. Impurities such as moisture originally present in the reactants may promote the formation of hydroxychlorides. The pale green color of the CuCl reactants indicated the possible presence of impurities. The grade of reactants was expected to better reflect conditions during regular operation and it was preferred for sets of experiments over an analytical grade of CuCl. The results indicated that the presence of hydroxychlorides was out of the XRD composition analysis detection range.

The forward reaction for oxygen production is endothermic, so its reverse reaction is exothermic. However, this does not imply that no external heat is required for the reactor because the reactants, i.e., CuCl and O₂, must be heated to the reaction temperature. Heat losses to the environment must be offset to maintain accuracy of the reaction temperature. Moreover, if the extent of the reverse reaction is not significant, the released heat from the reaction may not be sufficient to sustain the reaction temperature. In the experiments in this paper, the heating profiles of the reactor were obtained and studied to characterize the reaction temperature.

In the experiments, molten CuCl in the reactor is operated in a batch mode where no species are fed or removed during the time of the experiment. By comparison, oxygen flows continuously as bubbles through the molten CuCl. Due to the large density difference of molten CuCl and oxygen, the species would remain separated from each other if oxygen and CuCl are confined within the reactor with no feeding/removal during the experiment. The feeding and removal rates of oxygen are balanced, so the oxygen quantity in the reactor is kept at a constant value. If there is no product observed within the period of the experiment, the reverse reaction is insignificant.

3. Thermodynamic analysis of the reverse reaction

The reverse reaction in the decomposition of copper oxychloride occurs as follows:



The spontaneity of the reaction in Eq. (6) can be predicted from the change of the Gibbs free energy of the reaction, $\Delta_r^T G$. Any deviation from standard conditions can influence the behavior of the reaction. The reaction Gibbs free energy $\Delta_r^T G$ can be calculated as follows:

$$\Delta_r^T G = \Delta_r^T G^\circ + RT \ln(Q_r) \quad (7)$$

where $\Delta_r^T G^\circ$ is the change of Gibbs free energy of the reaction at standard pressure and temperature, and Q_r is the reaction quotient defined by the stoichiometric ratio of the product and reactant fugacity. Since CuCl and Cu₂OCl₂ in Eq. (6) exist in the form of a condensed state, the reaction quotient can be simplified by:

$$Q_r = \frac{1}{(P_{\text{O}_2}/P^\theta)^{1/2}} \quad (8)$$

where Q_r represents the reaction quotient, P^θ is the standard pressure (100 kPa) and P_{O_2} is the partial pressure of O₂ under actual reaction conditions. When the reaction reaches equilibrium, the quotient is equal to the reaction equilibrium constant K as defined by:

$$\Delta_r^T G^\circ = -RT \ln K \quad (9)$$

and K is then determined by:

$$K = Q = \frac{1}{(P_{\text{O}_2}/P^\theta)^{1/2}} \quad (10)$$

Here $\Delta_r^T G^\theta$ in Eq. (7) can be calculated from the molar Gibbs free energy of formation of the product and reactants:

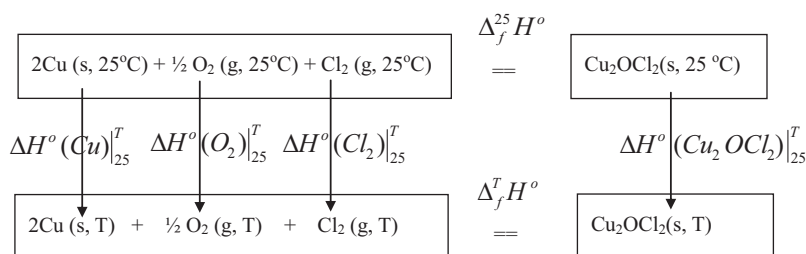
$$\Delta_r^T G^\circ = \Delta_f^T G^\circ(\text{Cu}_2\text{OCl}_2) - [2\Delta_f^T G^\circ(\text{CuCl}) + 1/2\Delta_f^T G^\circ(\text{O}_2)] \quad (11)$$

where $\Delta_f^T G^\circ(\text{Cu}_2\text{OCl}_2)$ and $\Delta_f^T G^\circ(\text{CuCl})$ are the molar Gibbs free energy of formation for CuCl and Cu₂OCl₂, respectively. The Gibbs free energy of formation of each reactant and product can be calculated from their enthalpy and entropy of formation:

$$\Delta_f^T G^\circ = \Delta_f^T H^\circ - T\Delta_f^T S^\circ \quad (12)$$

where $\Delta_f^T H^\circ$ and $\Delta_f^T S^\circ$ are the standard enthalpy and entropy of formation at temperature T . Unfortunately few data of $\Delta_f^T H^\circ$ and $\Delta_f^T S^\circ$ have been reported for CuCl and Cu₂OCl₂ in the temperature range of 400–550°C. CuCl exists in the solid phase up to the temperature of 412°C. At this temperature, it remains solid with a different microstructure and thermophysical properties. This phase is identifiable between the temperatures of 412 and 423°C. Beyond this temperature, CuCl remains liquid in the range of temperatures of interest with significant vaporization beyond the temperature of 550°C. The thermophysical properties of Cu₂OCl₂ are calculated from the properties of compounds and elements. The procedure utilizes known data of enthalpy and entropy at ambient temperature. For the product Cu₂OCl₂ in Eq. (6), the following schematic of a thermodynamic method is used for the

calculation of $\Delta_f^T H^\circ$:



The method also applies to the calculation of $\Delta_f^T S^\circ$, then

$$\begin{aligned}
 \Delta_f^T H^\circ &= [\Delta_f^{25} H^\circ + \Delta H^\circ(\text{Cu}_2\text{OCl}_2)_{25}^T] - [\Delta H^\circ(\text{Cu})_{25}^T \\
 &\quad + \Delta H^\circ(\text{O}_2)_{25}^T + \Delta H^\circ(\text{Cl}_2)_{25}^T] \quad (13)
 \end{aligned}$$

$$\begin{aligned}
 \Delta_f^T S^\circ &= [\Delta_f^{25} S^\circ + \Delta S^\circ(\text{Cu}_2\text{OCl}_2)_{25}^T] - [\Delta S^\circ(\text{Cu})_{25}^T \\
 &\quad + \Delta S^\circ(\text{O}_2)_{25}^T + \Delta S^\circ(\text{Cl}_2)_{25}^T] \quad (14)
 \end{aligned}$$

where the enthalpy and entropy changes for each component are calculated based on the following equations:

$$\Delta_{25}^T H^\circ = \int_{25}^T C_p dT \quad (15)$$

$$\Delta_{25}^T S^\circ = \int_{25}^T \frac{C_p dT}{T} \quad (16)$$

A similar methodology is adopted for the reactants CuCl and O₂ in Eq. (6) for the calculation of $\Delta_f^T H^\circ$ and $\Delta_f^T S^\circ$. The transition of CuCl, correlations of C_p and the values of $\Delta_f^{25} H^\circ$ for Cu, O₂, Cl₂ and CuCl reported by NIST [17] are adopted in this paper. The reactant CuCl experiences a phase change from solid to liquid at the temperature of 430 °C (803.15 K). The entropy change ΔS at the melting point is calculated with the following equation:

$$\Delta_{\text{melting}} S^\circ = \frac{\Delta H^\circ_{\text{melting}}}{803.15} \quad (17)$$

where ΔH represents the enthalpy of phase change. For Cu₂OCl₂, only the experimental data of specific heat capacity at constant pressure C_p in the temperature range of 25–410 °C was reported [18]. In this paper, the following equation is proposed to correlate the data:

$$C_p(\text{Cu}_2\text{OCl}_2) = 99.23243 + 0.021622 T \quad (18)$$

where C_p and T have units of J/mol K and K, respectively. The relative standard deviation of Eq. (18) in the temperature range of 25–410 °C is within 3%, so it will be assumed to be extended to the temperature of 550 °C.

The thermodynamic properties for the formation of Cu₂OCl₂ and CuCl, i.e., values of $\Delta_f^T H^\circ$, $\Delta_f^T S^\circ$ and $\Delta_f^T G^\circ$, calculated from Eqs. (11), (13) and (14), follow the thermodynamic method described above (shown in Table 2). Based on these thermodynamic properties, the changes of standard enthalpy $\Delta_f^T H^\circ$, entropy $\Delta_f^T S^\circ$, and Gibbs free energy $\Delta_f^T G^\circ$ for the reaction in Eq. (6) can be calculated, as shown in Figs. 3–5. The negative values of the reaction enthalpy in the temperature range of reactions as shown in Fig. 3 indicate that the reverse reaction is exothermic. The steep slope at 430 °C is explained by the phase change of CuCl at this temperature, which also explains the steep slope for the standard entropy of reaction, as shown in Fig. 3. This sudden change does not exist in Fig. 4 for the standard Gibbs free energy $\Delta_f^T G^\circ$ because the phase change of CuCl is close to a reversible thermodynamic process under isobaric conditions.

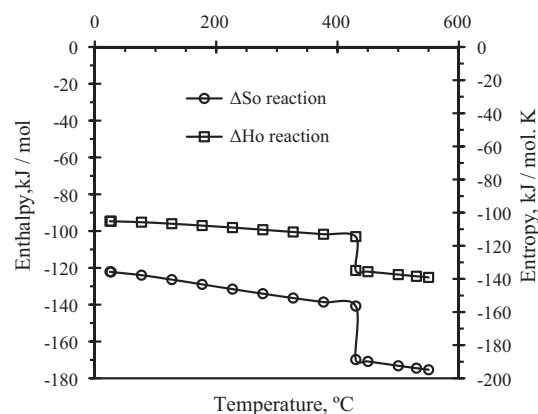


Fig. 3. Standard enthalpy ($\Delta_f^T H^\theta$) and entropy ($\Delta_f^T S^\theta$) of the reverse reaction at various temperatures.

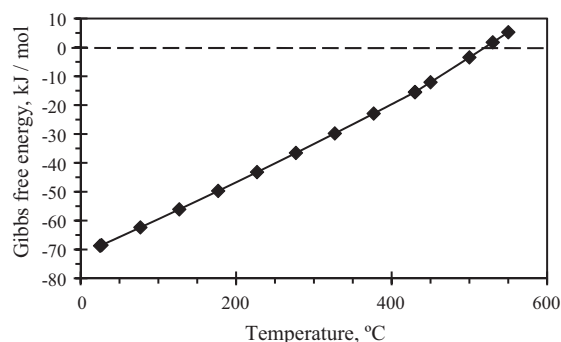


Fig. 4. Standard Gibbs free energy ($\Delta_f^T G^\theta$) of the reverse reaction at various temperatures.

As indicated in Fig. 4, the transitional point from negative to positive Gibbs free energy $\Delta_f^T G^\circ$ occurs close to 520 °C, which indicates that the reverse reaction is spontaneous if the temperature is below 520 °C at standard pressure, or the reaction will not occur when the temperature is higher than 520 °C at standard pressure.

Fig. 5 shows the calculation results for the operating pressure range of 1.0×10^{-10} to 100 bar to represent the range of vacuum to highly pressurized reactors. An analysis of Fig. 5 indicates that the reverse reaction may be minimized by either decreasing the oxygen pressure or increasing the reaction temperature. When the oxygen pressure is decreased to below 1 bar, a vacuum will be created. Since the produced oxygen in the forward reaction is often pressurized for further storage or utilization in other units that consume oxygen, a vacuum oxygen production reactor may increase the power consumption of the vacuum and pressurization for industrial scale oxygen production. In addition, a vacuum is more likely than pressurization to introduce other gases into the oxygen production reactor. Furthermore, negative pressure may also increase the

Table 2
Thermodynamic properties for the formation of Cu_2OCl_2 and CuCl .

T (°C)	Cu_2OCl_2			CuCl		
	$\Delta_f^T H^\theta$ (kJ/kmol)	$\Delta_f^T S^\theta$ (kJ/kmol K)	$\Delta_f^T G^\theta$ (kJ/kmol)	$\Delta_f^T H^\theta$ (kJ/kmol)	$\Delta_f^T S^\theta$ (kJ/kmol K)	$\Delta_f^T G^\theta$ (kJ/kmol)
25	-381,286	-237.453	-310,486	-138,069	-57.665	-120,885
27	-381,284	-237.444	-310,047	-138,055	-57.617	-120,770
77	-380,897	-236.251	-298,205	-137,578	-56.155	-117,924
127	-380,539	-235.293	-286,417	-136,946	-54.472	-115,158
177	-380,200	-234.494	-274,672	-136,224	-52.772	-112,477
227	-379,872	-233.804	-262,965	-135,446	-51.134	-109,879
277	-379,550	-233.190	-251,289	-134,634	-49.586	-107,362
327	-379,227	-232.627	-239,644	-133,799	-48.133	-104,919
377	-378,897	-232.100	-228,025	-132,948	-46.771	-102,547
430	-378,520.4	-231.735	-215,703	-132,025	-45.406	-100,098
430 ^a	-378,520.4	-231.735	-215,703	-121,814	-30.873	-100.106
450	-378,393	-231.364	-211,074	-121,392	-30.282	-99,494
500	-378,027	-230.878	-199,515	-120,332	-28.863	-98,016
530	-377,798	-230.591	-192,589	-119,702	-28.064	-97,162
550	-377,640	-230.402	-187,976	-119,285	-27.552	-96,606

^a CuCl changes from solid to liquid at 430 °C.

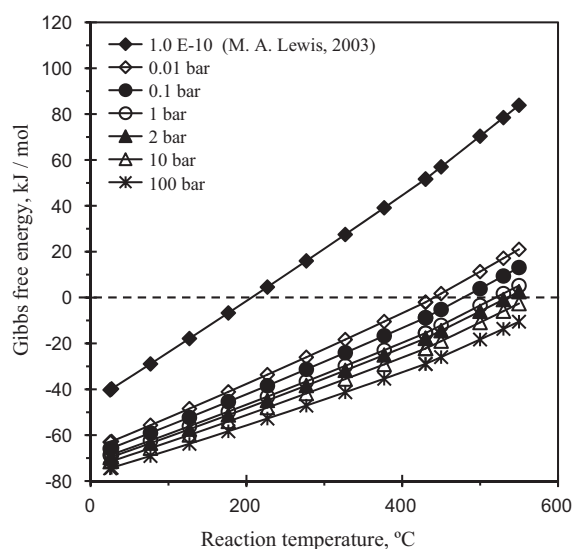


Fig. 5. Gibbs free energy of the reverse reaction at various operating conditions.

generation of CuCl vapor. Therefore, a vacuum oxygen production reactor is not suggested for the Cu – Cl cycle.

A method of minimizing the reverse reaction is to increase the operating temperature. If the temperature is higher than 530 °C, significant amounts of CuCl vapour may be generated, as observed in the reactor and oxygen outlet in the experiments. Fig. 6 shows the vapor pressure of CuCl based on experimental data reported in

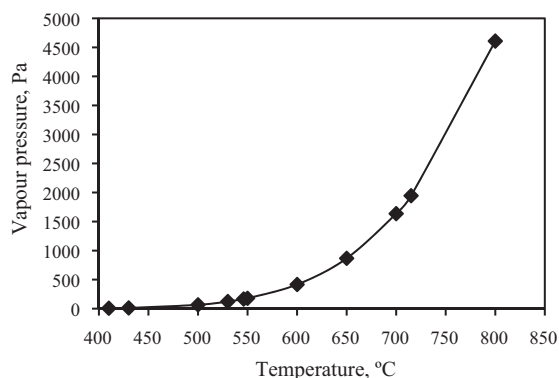


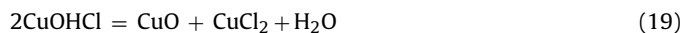
Fig. 6. Vapor pressure of CuCl at various different temperatures.

previous studies [18–22]. The temperature must be below 550 °C in order to maintain the vapor pressure of CuCl below 1000 Pa (0.01 bar). For CuCl vapor minimization and the simultaneous impact of pressure and temperature on the Gibbs free energy, the optimum operating pressure is suggested in the range of 1–2 bar and a temperature in the range of 525–550 °C. Although it is desirable to decompose Cu_2OCl_2 at lower temperatures, experimental results of decomposition of copper oxychloride indicate that the conversion rate is very low below 500 °C [12]. As shown in Fig. 5, the Gibbs free energy of the reverse reaction is slightly above zero at temperatures in the range of 525–550 °C.

Fig. 5 also indicates that the reverse reaction is spontaneous when the operating temperature is below 450 °C, and the oxygen pressure is higher than 0.01 bar. This implies the reverse reaction may occur in the process of reactant preheating from a temperature significantly lower than 450 °C to a temperature higher than 450 °C, as indicated by the temperature difference of the hydrolysis step and its downstream oxygen production step shown in Table 1.

4. Results and discussion

Table 3 summarizes the experimental results and reaction conditions. In order to have significant mixing and enhance the contact of O_2 and CuCl , 2–3 times of oxygen quantity in excess of the stoichiometric balance was adopted in the experiments. The operating time of each experiment was at least one hour. Two temperatures were examined: 450 °C, just above the melting point of CuCl , and 500 °C, close to the transitional point of the Gibbs free energy of the reaction. The implications of different temperatures will be discussed based on results of X-ray powder diffraction analysis (XRD). Figs. 7–10 show the XRD results that correspond to experiments No. 1–4 of Table 3. It can be found that no Cu_2OCl_2 was produced in all experiments that operated in the temperature range of 450–500 °C, although experiment No. 3 resulted in some produced CuO . As to the formation of CuO in experiment No. 3, it is believed that CuO may have been generated from moisture in the reactant CuCl during the preparation process because the purity of reactant CuCl is larger than 99%, but the CuO detected in the product is 5%. The composition of the reactant CuCl for experiment No. 3 was analyzed to determine the level of impurity. As shown in Fig. 10, the only impurity in CuCl was found to be CuOHCl , which may generate CuO through the following reaction [23–25]:



CuCl_2 is then decomposed to CuCl and oxygen. It is believed that the hydrogen element in CuOHCl occurred from moisture due to the

Table 3
Experimental conditions and results for the reaction of CuCl and O₂.

No.	T (°C)	Reactants purity ^a (%)	Runtime (h)	Ratio of total quantity ^b (O ₂ /CuCl)	Pressure (bar)	Inlet oxygen concentration (mole fraction)	Oxygen decrease in reaction (mole)	Composition of product (by XRD) % (±3%)
1	450	99%	1	1.3	1.2	5%	0	CuCl
2	500	99%	1	1.3	1.2	5%	0	CuCl
3	500	99%	1	1.3	1.2	5%	0	5 wt.% CuO 95 wt.% CuCl
4 ^c	500	99%	1	–	1.2	–	–	97% CuCl 3% Cu(OH)Cl

^a All sets of experiments used 0.5 mol of reactant and continuous air injection at 2 SLPM.

^b The stoichiometric ratio of O₂ to CuCl is 0.5.

^c Baseline experiments with continuous nitrogen flow at 2 SLPM.

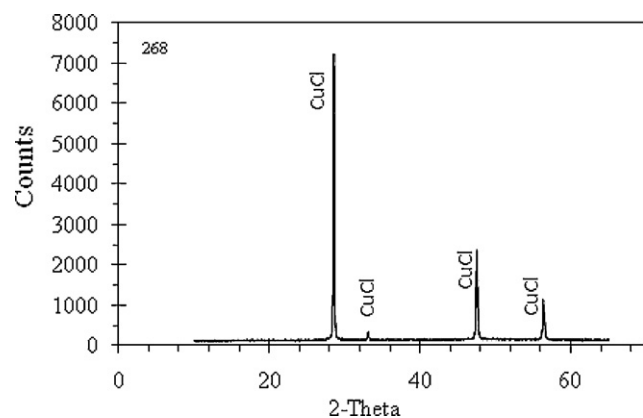


Fig. 7. XRD results of products of CuCl+O₂ at 450 °C, 1-h test (experiment #1 in Table 2).

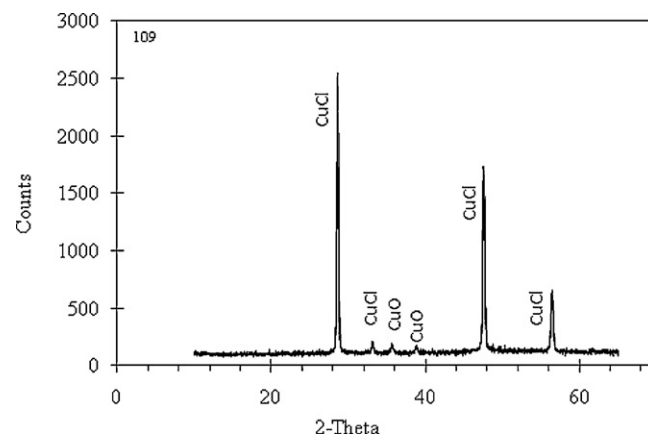


Fig. 9. XRD results of CuCl and O₂ at 500 °C, 1-h test (experiment #3 in Table 2).

presence of humidity when preparing the CuCl sample. It is unclear how the CuOHCl was formed in the CuCl during the process. This will be studied in future investigations.

From the experimental results, it can be concluded that the reverse reaction as described in Eq. (6) has little likelihood to occur under the conditions reported in Table 3. The low likelihood of the reverse reaction to occur can be the result of two factors. First, the reverse reaction is not thermodynamically spontaneous, and second, the reverse reaction is spontaneous, but the runtime for the reverse reaction is not long enough to produce significant amounts of Cu₂OCl₂. If the reverse reaction is spontaneous, then the run time must be very long, or the equipment size must be very large for the reverse reaction to produce measurable amounts of Cu₂OCl₂.

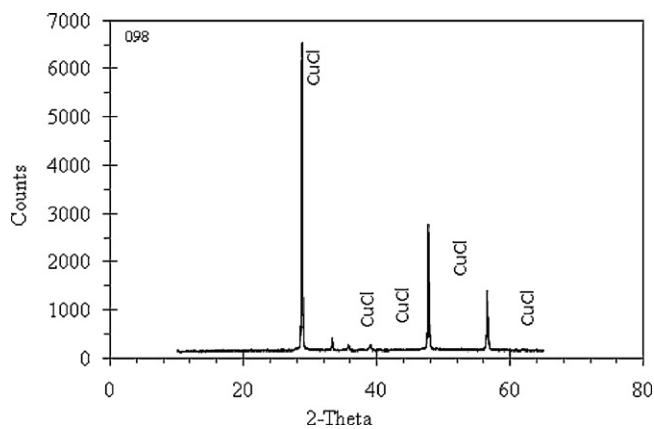


Fig. 8. XRD results of products of CuCl+O₂ at 500 °C, 1 h test (experiment #2 in Table 2).

The standard Gibbs free energy of the reverse reaction shown in Fig. 4 suggests the spontaneity of the reaction in the temperature range. This does not conflict with the experimental results because the oxygen partial pressure in the experiments was below the standard value. As shown in Table 3, the partial pressure of O₂ in the experiments was far below 1 bar, which may significantly lower the possibility of a reverse reaction based on the Gibbs free energy. This observation also suggests that the reverse reaction may be a function of the oxygen pressure in the reactor. When the operating pressure of oxygen is different from the standard pressure, the Gibbs free energy of the reverse reaction at various pressures can be calculated from Eq. (7).

The reverse reaction was not observed in the preheating of CuCl and O₂, in the experiments, although Fig. 5 shows negative values of the Gibbs free energy when the operating pressure (0.06 bar) is much higher than 0.01 bar. The XRD reflections (see Figs. 7–10)

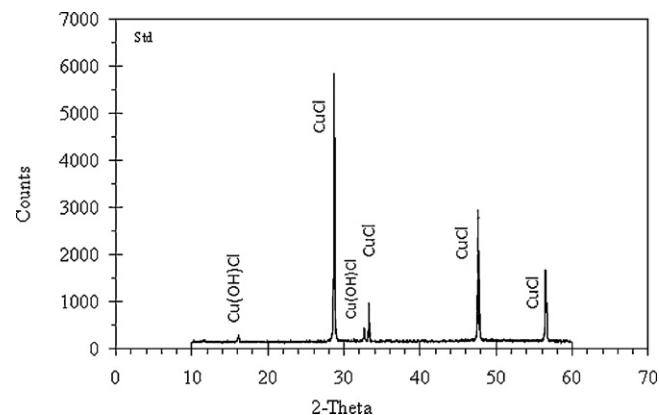


Fig. 10. Impurities in the CuCl reactant, molten at 500 °C (experiment #4 in Table 2).

did not show any trace of Cu_2OCl_2 . Several conditions can lead to these results, for example, the reverse reaction below 450°C is too slow to be measured. The sensitivity of the oxygen sensor and XRD may not be sufficient to detect the composition change. Also, the reverse reaction did take place, as suggested by the negative value of Gibbs free energy, and Cu_2OCl_2 was produced, but after heating to $450\text{--}500^\circ\text{C}$, the Cu_2OCl_2 decomposed back to CuCl and O_2 , as indicated in Fig. 5 by the positive value of Gibbs energy within the temperature range. Under 430°C , CuCl exists in the form of solid, and the mixing of oxygen and CuCl is not sufficient to facilitate the reverse reaction. This condition may also prevail in the mixture of molten CuCl and oxygen. Under normal operating conditions of 1–2 bar and $525\text{--}550^\circ\text{C}$, and within the reaction time of interest, the reverse reaction can be neglected in the design and operation of the oxygen production reactor of the Cu–Cl cycle.

5. Conclusions

This paper presented an experimental study of a potential reverse reaction of oxygen production in the Cu–Cl thermochemical cycle. The operating conditions that disfavor the reverse reaction were examined. The analysis of the products with XRD analysis indicated that the reverse reaction did not occur at temperatures in the range of $450\text{--}500^\circ\text{C}$, and oxygen pressures below 2 bar. The presence of humidity should be avoided in the reaction system so as to avoid undesirable products such as CuOHCl and CuO . The thermochemistry data of Cu_2OCl_2 and CuCl at various temperatures in the reaction system were calculated. Thermodynamic methods were designed in order to utilize the data of standard conditions, low temperatures, and elementary species. The data included the standard entropy, enthalpy and Gibbs free energy of formation at different temperatures. A thermodynamic analysis was also performed to study the spontaneity of the reverse reaction under various operating conditions. The combined effects of pressure and temperature on the Gibbs free energy of the reaction indicated that the optimum operating conditions correspond to pressures in the range of 1–2 bar, and temperatures within $525\text{--}550^\circ\text{C}$. In these temperature ranges, the Gibbs free energy of the reverse reaction has positive values. Although a vacuum or high temperature also disfavors the reverse reaction, in this paper, they are not recommended as the operating conditions in a scaled-up installation would be challenging due to oxygen storage, as well as significant CuCl vapor under those conditions, and the additional energy consumption implications. It is concluded that the decomposition of copper oxychloride occurs when operating at pressures of 1–2 bar and temperatures of $525\text{--}550^\circ\text{C}$. Therefore, the reverse reaction of oxygen production can be neglected in the design and operation of the Cu–Cl cycle.

Acknowledgments

Financial support of this research from Atomic Energy of Canada Limited and the Ontario Research Excellence Fund is appreciated, as well as helpful input from Dr. Venkata Dagupatti.

References

- [1] B.W. McQuillan, L.C. Brown, G.E. Besenbruch, R. Tolman, T. Cramer, B.E. Russ, B.A. Vermillion, High efficiency generation of hydrogen fuels using solar thermochemical splitting of water, General Atomics, Report GA-A24972.
- [2] R.H. Carty, M.M. Mazumder, J.D. Schreiber, J.B. Pangborn, Thermochemical Hydrogen Production, Institute of Gas Technology, 1981, GRI-80-0023.
- [3] M.A. Lewis, A Taylor, High temperature thermochemical processes, DOE Hydrogen Program, Annual Progress Report (2006) 182–185.
- [4] M. Sakurai, H. Nakajima, R. Amir, K. Onuki, S. Shimizu, Experimental study on side-reaction occurrence condition in the iodine-sulfur thermochemical hydrogen production process, *International Journal of Hydrogen Energy* (2000) 613–619.
- [5] K. Schultz, Technical Report for the Stanford Global Climate and Energy Project, General Atomics, Thermochemical production of hydrogen from solar and nuclear energy, Technical Report for the Stanford Global Climate and Energy Project, General Atomics (2003).
- [6] C. Zamfirescu, G.F. Naterer, I. Dincer, Vapor compression CuCl heat pump integrated with a thermochemical water splitting plant, *Thermochimica Acta* 512 (2011) 40–48.
- [7] V.N. Daggupati, G.F. Naterer, I. Dincer, Convective heat transfer and solid conversion of reacting particles in a copper (II) chloride fluidized bed, *Chemical Engineering Science* 66 (2011) 460–468.
- [8] Y. Haseli, I. Dincer, G.F. Naterer, Hydrodynamic gas–solid model of cupric chloride particles reacting with superheated steam for thermochemical hydrogen production, *Chemical Engineering Science* 63 (2008) 4596–4604.
- [9] C. Lamberti, C. Prestipino, L. Capello, S. Bordiga, A. Zec, G. Spotto, S. Diaz, A. Marsella, B. Cremaschi, M. Garilli, S. Vidotto, G. Leofanti, The $\text{CuCl}_2/\text{Al}_2\text{O}_3$ catalyst investigated in interaction with reagents, *International Journal of Molecular Science* 2 (2001) 230–245.
- [10] T. Parry, Thermodynamics and Magnetism of Cu_2OCl_2 , Department of Chemistry and Biochemistry, Brigham Young University, 2008.
- [11] M.A. Lewis, M. Serban, J.K. Basco, Hydrogen production at $<550^\circ\text{C}$ using a low temperature thermochemical cycle, in: Proceedings of the Nuclear Production of Hydrogen: Second Information Exchange Meeting, Argonne, IL, USA, 2–3 October, 2003, pp. 145–156.
- [12] M. Serban, M.A. Lewis, J.K. Basco, Kinetic study of the hydrogen and oxygen production reactions, in: AIChE 2004 Spring National Meeting, 2004.
- [13] ASME International, Policy on reporting uncertainties in experimental measurements and results, *Journal of Heat Transfer Policy* 115 (1993) 5–6.
- [14] Introduction to X-ray diffraction. PANalytical. [Online] Speciris, 2010. [Cited: September 09, 2010.] <http://www.panalytical.com/index.cfm?pid=135>.
- [15] H.P. Alexander, L.E. Klug, X-ray Diffraction Procedures for Polycrystalline and Amorphous Materials, John Wiley & Sons, 1975.
- [16] J. Leroux, D.H. Lennox, K. Kay, Direct quantitative X-ray analysis by diffraction-absorption techniques, *Journal of Analytical Chemistry* 25 (1953) 740–743.
- [17] National Institute of Standards and Technology. Chemistry WebBook. [Online] NIST, February 1, 2010. [Cited: October 5, 2010.] <http://webbook.nist.gov/chemistry/>.
- [18] L. Brewer, N.L. Lofgren, The thermodynamics of gaseous cuprous chloride, monomer and trimer, *Journal of the American Chemical Society* 72 (1950) 3038.
- [19] M. Guido, G. Gigli, M. Spoliti, Mass spectrometric study of the vaporization of cuprous chloride and the dissociation energy of Cu_3Cl_3 , Cu_4Cl_4 , and Cu_5Cl_5 , *Journal of Chemical Physics* 55 (1971) 4566.
- [20] M. Guido, G. Gigli, G.I. Balducci, Dissociation energy of CuCl and Cu_3CuCl_3 gaseous molecules, *Journal of Chemical Physics* 57 (1972) 3731.
- [21] L.C. Wagner, P. Robert, Q. Grindstaff, I. Grimley, Mass spectrometric study of the fragmentation of the cuprous chloride vapor system, *Journal of Mass Spectrometry* 15 (1974) 255.
- [22] S. Mizuno, K. Nakayama, T. Kawachi, Y. Kojima, F. Watanabe, H. Matsuda, M.1. Takada, Enhancement of chloride volatilization of Zn, Pb and Cu from molten fly ash under reduced pressure, *The Society of Chemical Engineers (Japan)* 32 (2006) 99–102.
- [23] P. Ramamurtahyde, A. Secco, Studies on metal hydroxyl compounds. IX. Kinetics of thermal decomposition of twelve copper halide derivatives, *Canadian Journal of Chemistry* 47 (1969) 3915–3918.
- [24] P. Ramamurtahyde, A. Secco, Addendum: studies on metal hydroxyl compounds, Heats of decomposition of twelve copper halide derivatives, *Canadian Journal of Chemistry* 47 (1969) 2303–2304.
- [25] P. Ramamurtahyde, A. Secco, Studies on metal hydroxyl compounds. VII. Thermal analyses of copper derivatives, *Canadian Journal of Chemistry* 47 (1969) 2185–2190.